Brain Stimulation 13 (2020) 1743–1752

Contents lists available at ScienceDirect

Brain Stimulation

journal homepage: http://www.journals.elsevier.com/brain-stimulation

Gait-related frequency modulation of beta oscillatory activity in the subthalamic nucleus of parkinsonian patients

Andrea Canessa [a, b], Chiara Palmisano [a], Ioannis U. Isaias [a, *, 1], Alberto Mazzoni [c, 1]

[a] Department of Neurology, University Hospital and Julius Maximilian University, Würzburg, Germany
[b] Department of Informatics, Bioengineering, Robotics and System Engineering, University of Genoa, Genoa, Italy
[c] The BioRobotics Institute and Department of Excellence of Robotics and AI, Scuola Superiore Sant'Anna, Pisa, Italy

ARTICLE INFO

Article history:
Received 26 August 2020
Accepted 13 September 2020
Available online 19 September 2020

Keywords:
Adaptive deep brain stimulation
Gait
Local field potentials
Parkinson's disease
Subthalamic nucleus

ABSTRACT

Background: Abnormal beta band activity in the subthalamic nucleus (STN) is known to be exaggerated in patients with Parkinson's disease, and the amplitude of such activity has been associated with akinetic rigid symptoms. New devices for deep brain stimulation (DBS) that operate by adapting the stimulation parameters generally rely on the detection of beta activity amplitude modulations in these patients. Movement-related frequency modulation of beta oscillatory activity has been poorly investigated, despite being an attractive variable for extracting information about basal ganglia activity.
Objective: We studied the STN oscillatory activity associated with locomotion and proposed a new approach to extract movement related information from beta band activity.
Methods: We recorded bilateral local field potential of the STN in eight parkinsonian patients implanted with DBS electrodes during upright quiet standing and unperturbed walking. Neurophysiological recordings were combined with kinematic measurements and individual molecular brain imaging studies. We then determined the information carried by the STN oscillatory activity about locomotion and we identified task-specific biomarkers.
Results: We found a gait-related peak frequency modulation of the beta band of STN recordings of parkinsonian patients. This novel biomarker and the associated power modulations were highly informative to detect the walking state (with respect to standing) in each single patient.
Conclusion: Frequency modulation in the human STN represents a fundamental aspect of information processing of locomotion. Our information-driven approach could significantly enrich the spectrum of Parkinson's neural markers, with input signals encoding ongoing tasks execution for an appropriate online tuning of DBS delivery.
© 2020 The Author(s). Published by Elsevier Inc. This is an open access article under the CC BY-NC-ND license (http://creativecommons.org/licenses/by-nc-nd/4.0/).

Introduction

The use of deep brain stimulation (DBS) to intervene directly in pathological neural circuits has changed the way we treat brain diseases and investigate their underlying pathophysiology. However, more than two decades after its introduction as a treatment for motor symptoms of Parkinson's disease (PD), DBS is still associated with drawbacks, including limited efficacy and adverse effects. For example, stimulation at the most commonly used targets – the subthalamic nucleus (STN), the globus pallidus internus (GPi) or the motor thalamus – does little to improve (or can even exacerbate) gait disturbances [1–4].

Most DBS systems in current use are open-loop devices. They provide continuous stimulation (cDBS) regardless of the (task-related) state of neural activity or its symptom-specific derangements. By contrast, new DBS systems being developed operate by adapting the stimulation parameters (such as amplitude and frequency) in response to an input signal (adaptive DBS, aDBS) [5–7]. The most studied input signal to control aDBS in PD relies on the analysis of oscillations in local field potentials (LFP) in the dorsolateral (motor) territory of the STN. Excessive oscillations in the beta frequency range [13,35]Hz are consistently recorded over time by the stimulating electrodes of unmedicated PD patients in a resting state condition [8]. Although a definitive demonstration of causality is lacking, the relationships between excessive

* Corresponding author. University Hospital of Würzburg, Josef-Schneider-Straße 11, D-97080, Würzburg, Germany.
E-mail address: Isaias_I@ukw.de (I.U. Isaias).
[1] These authors share same senior author contribution.

https://doi.org/10.1016/j.brs.2020.09.006
1935-861X/© 2020 The Author(s). Published by Elsevier Inc. This is an open access article under the CC BY-NC-ND license (http://creativecommons.org/licenses/by-nc-nd/4.0/).

subthalamic oscillatory activity and the severity of akinetic-rigid symptoms [8] and between beta amplitude suppression and the effectiveness of levodopa therapy [9] or cDBS [10] further supported the use of the power of beta oscillations as a biomarker for PD [8,11–13].

However, caution is warranted in using beta oscillations for aDBS, as they are relevant for many perceptual, cognitive, and motor physiological processes [14]. Indeed, while ameliorating certain symptoms, power beta modulation might impair the residual task-related physiological coding capacity of the stimulated area [15]. Furthermore, amplitude modulation might not capture circuit dynamics, such as frequency- and phase-specific synchronization [16,17], which would be fundamental in routing the information flow across distant brain areas [18,19]. This might be particularly the case for large-scale networks such as the locomotor network [20,21].

In this study, we investigated the beta modulations associated with locomotion in the STN of eight parkinsonian patients and identified beta-related neural features able to reliably discriminate between the standing and walking conditions in each single patient.

Methods

Subjects, surgery, clinical and molecular imaging evaluation

We tested eight patients with idiopathic PD according to the UK Parkinson Disease Brain Bank criteria [22]. Additional inclusion criteria were a stable clinical response to STN DBS, with unchanged parameters and medications for at least eight weeks prior to the study. Exclusion criteria were any other neurological disorder including cognitive decline or mood disturbances, as evaluated using standardized rating scales (i.e., Parkinson neuropsychometric dementia assessment, Mattis dementia rating scale, Hamilton depression rating scale, and the non-motor symptoms scale), diabetes, and orthopedic problems. A preoperative 3 T MRI (T1, T2, T2*, FLAIR, Trio, Siemens Medical Systems) ruled out morphological anomalies.

All patients were implanted at the University Hospital of Würzburg (Würzburg, Germany) with the Activa PC+S® system (Medtronic, PLC). This system allows therapeutic DBS as well as on-demand LFP recordings from the chronically-implanted electrodes. The device and the related hardware and software for programming and readout were provided by Medtronic PLC under a request for application agreement. The company had no impact on study design, patient selection, data analysis, or reporting of the results.

The surgical procedure has been previously described [4,23]. All patients received quadripolar macroelectrodes (model 3389, Medtronic PLC). The intended coordinates for the STN (i.e., 12mm lateral, 2mm posterior, 4mm ventral to the mid-commissural point) were adjusted according to individual delineation of the STN on T2-weighted and susceptibility-weighted MRI (Siemens MAGNETOM Trio 3.0 T). The precise localization of the active (and recording) contacts in the STN was confirmed by image fusion of preoperative stereotactic MRI and postoperative CT scans (SureTune™, Medtronic, PLC) [4,24].

For clinical assessment, parkinsonian patients were evaluated within one month before surgery (pre-DBS) with the Unified Parkinson's Disease Rating Scales motor score (UPDRS-III) after overnight (>12h) withdrawal of all dopaminergic medications (meds-off) and about 1h upon receiving 1 to 1.5 times levodopa/benserazide of the levodopa-equivalent morning dose (meds-on). After surgery (post-DBS), patients were clinically assessed using the UPDRS-III with: (i) stimulation off for at least 2 h (stim-off), (ii) stimulation on (stim-on) with the clinically optimized and chronically used stimulation parameters, (iii) meds-on (as before surgery), and (iv) meds-on and stim-on. The stimulation parameters were controlled by a physician independent from our study, which provided sustained improvement without any side effects.

All patients performed a single-photon computed tomography (SPECT) and [^{123}I]N-ω-fluoropropyl-2β-carbomethoxy - 3β -(4-iodophenyl)nortropane (FP-CIT) to measure the striatal dopamine reuptake transporters (DAT) density. SPECT data acquisition and analysis have been described previously [25,26]. Striatal DAT binding measurements of the patients were compared with normal values of 15 healthy subjects (four males; age, mean and standard deviation (SD) 62±9 years, range [44; 68] years) (Supp. Table 1). Based on the non-displaceable binding potential (BP_{ND}) of the DAT, we identified the STN of the brain hemisphere with more (+) or less (−) dopaminergic innervation [7,24].

The local Institutional Review Board of the University Hospital of Würzburg approved the study and all patients gave written informed consent according to the Declaration of Helsinki.

Protocol and biomechanical assessment

The gait analysis was performed in the morning in the meds-off and stim-off condition. Subjects walked barefoot at their preferred speed over a 7m long walkway. At the beginning of each walking trial, we recorded about 30s of quiet upright standing. Subjects started walking after a verbal cue. Patients performed at least six trials (range six to ten) according to their clinical conditions.

Kinematic data were recorded using an optoelectronic system (SMART-DX, BTS) and 29 spherical retro-reflective markers (15mm diameter) fixed to anatomical landmarks [27]. The gait cycle (i.e., the stride) was characterized by a set of parameters automatically extracted with MatLab-based custom scripts (Matlab 2019, The MathWorks, Inc) and visually inspected [28].

The stride is the interval between two sequential initial floor contacts by the same limb (i.e., the heel strike of one foot and the next heel strike of the same foot). We measured the stride duration, length, and velocity (normalized to subject's height), as well as the stance and double-support duration (time-normalized as a percentage of the stride duration). For each subject and condition, all variables were averaged over the trials. Normative data were obtained with the same experimental setup from 11 healthy controls matched for age and anthropometric measurements (nine males; age, mean and SD 58±4.7 years, range [50; 66] years) (Supp. Table 2).

Electrophysiological signal recording and analysis

We recorded the LFP with single bipolar derivation, amplified by 1000, and sampled at 422Hz. We selected a bipolar montage crossing the chronically-active electrode [29].

The synchronization across devices was achieved with two transcutaneous electrical nerve stimulation (TENS) artefacts at the beginning and at the end of each trial, introduced simultaneously into the Activa PC+S® and the SMART-DX acquisition systems. The TENS electrodes were placed on the supraclavicular fossa, directly on the cable that connects the impulse generator with the electrodes, and over the burr-hole site. One electromyographic probe (FREEEMG, BTS), built-in with the SMART-DX, was placed next to the TENS electrodes. We used the last peak of each TENS artefact as the synchronization instant across modalities, easily recognizable because of its sharp drop-off.

The LFP recordings of two STNs (STN+ for wue09 and STN- for wue10) showed cardiac artefacts. In this case, we first detected signal peaks representing the QRS complex of the (synchronized) electrocardiogram. We then divided the LFP signals in epochs of 1s,

centered on each QRS peak time. We created a matrix N x time-frame (where N is the number of QRS peaks) and computed its singular value decomposition. To clean the LFP signal [30], we (i) visually detected all the eigenvectors corresponding to ECG artefact, (ii) reconstructed from these components the artefact signal, and (iii) subtracted from the original LFP signal the reconstructed artefact signal.

We analysed the LFP by means of a time-frequency decomposition using 46 Morlet wavelets in the [5;40]Hz range (central frequency = 1Hz, Full Width Half Maximum = 3s) [31]. The recordings during walking were divided into epochs corresponding to a stride (WALK [epochs]). Since the stride length varied across trials and subjects, we used a linear time-warp algorithm, similar to the one proposed by Sadeghi and coll [32] to normalize the time-frequency representation of each stride to a reference stride duration of 1.15s, which was equal to the mean stride duration of the whole patient population (Supp. Table 2). We used a third order polynomial interpolation with a 1.5s time-window centered at each velocity peak of the swing foot. This time window lasted 1.5s to exceed the duration of the stride, and ensured that the interpolation border-effect did not influence the analysis window. The number of WALK epochs in the whole study population was in the range [13;21]. In line with this approach, the LFP recordings of quietly upright standing (STAND [epochs]) were also divided in successive, non-overlapping epochs with the same duration of the reference stride (i.e., 1.15s). For each epoch, we then estimated the PSD integrating its time-frequency representation over time. We then computed the mean PSD for both STAND and WALK, averaging across epochs of the respective condition.

The LFP recordings were characterized by the simultaneous presence of an aperiodic background with 1/f PSD superimposed to the true oscillatory periodic components. To properly analyze specific power changes, we decided to parameterize the estimated mean PSD to disentangle this double aperiodic/periodic nature of LFP signal power [33]. Following Haller and coll. [33], we modeled the mean PSD as the sum of putative, periodic oscillatory components parameterized by their central frequency, power and bandwidth, as measured from Gaussian mixture model fits, plus an aperiodic component, as described from a power law fit (Supp. Fig. 1). Following the parameterization procedure, we removed the "colored" 1/f background noise from the PSD of each epoch to analyze only the true oscillatory components (Fig. 1). Unless otherwise specified, the PSD results discussed in the text were obtained after 1/f noise removal.

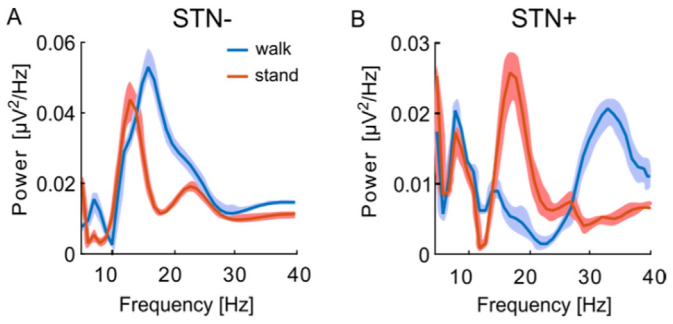

Fig. 1. Spectral peaks during the walking and standing condition of one patient (wue02).
A) Power spectral density of the subthalamic nucleus (STN) local field potentials after removal of the aperiodic component (see Methods) during standing (red line) and walking (blue line). Filled areas represent the standard error of the mean (SEM) computed as the 5% and 95% confidence intervals of the bootstrapped distribution across trials (100 repetitions with replacement). **B)** Same as (A) for the other STN (of the least dopamine-depleted hemisphere, STN+). (For interpretation of the references to color in this figure legend, the reader is referred to the Web version of this article.)

Information analysis

Mutual information [34] can quantify the reduction of uncertainty about a given external state that can be gained from observing a single-trial neural activity feature [35,36].

We evaluated for each subject how much information about the state or condition (i.e., STAND and WALK) was contained in different features of the subthalamic LFP spectrum during each epoch. Given a feature F having values r and a set of subject states S, the mutual information between F and S is given by (Eqn 1):

$$I(S;F) = \sum_{s} P(s) \sum_{r} P(r|s) \log_2 \frac{P(r|s)}{P(r)} \quad (1)$$

where $P(s)$ is the probability of being in the state s, $P(r|s)$ is the probability of observing in the same epoch a value r of the feature given a state s, and $P(r)$ is the probability of observing across all epochs a value r of the feature. Here, the set of possible states S was composed by two different conditions, S = {STAND, WALK}.

We considered the following six features (i-vi) of the subthalamic LFP spectrum. The first feature (i) was the frequency with the highest amplitude (f_{PEAK}) in the entire beta band [13;35]Hz in the PSD of each epoch. In the PSD parameterization, we selected the Gaussian component G (defined in terms of its amplitude A_G, center frequency f_G, and support σ_G) with the highest amplitude. We were thus able to define a dominant frequency peak for the STAND (f_{STAND}) and WALK (f_{WALK}) condition. Then we considered the power of each epoch, integrating the PSD of each STN, (ii) in the range f_{STAND}±2 Hz (P_{SF}), (iii) in the range f_{WALK}±2 Hz (P_{WF}), and (iv) for the entire beta band [13;35]Hz (P_{BETA}). The fifth (v) feature considered was the amplitude of the PSD at each frequency bin in the range [5;40]Hz, used to compute the amount of information carried by each bin (i.e., spectral information [37,38]). From the spectral information, we identified the most informative frequency (f_{MIF}) as the frequency bin showing the highest significant peak. The last feature (vi) was the power (P_{MIF}) of each epoch computed, integrating the PSD of each STN in the range f_{MIF}±2 Hz.

Each set of feature values was binned into four equipopulated bins to reduce information bias [39].

This single-feature information analysis (e.g., for P_{MIF} of the STN- and the STN+ separately) was then extended to compute how much information about the state was carried by the combination of features pairs (e.g., for P_{MIF} of the two hemispheres combined). The mutual information that the joint knowledge of the features F_1 and F_2 conveys about the states is defined as (Eqn 2):

$$I(S;F_1,F_2) = \sum_{s} P(s) \sum_{r_{1,2}} P(r_1,r_2|s) \log_2 \frac{P(r_1,r_2|s)}{P(r_1,r_2)} \quad (2)$$

In case of joint information, we also computed information redundancy (Eqn 3):

$$Red(S;F_1,\ F_2) = I(S;F_1) + I(S;F_2) - I(S;F_1,\ F_2) \quad (3)$$

which defines the amount of information about the state shared by the two features. When redundancy is less than the amount of information carried by each single feature, the two features convey some independent information. We corrected the bias in the information estimate due to the limited dataset using the Panzeri-Treves (PT) bias correction [40]. The significance of mutual information was computed with a bootstrap test, (significance if information >95% percentile of the information carried by randomized

data, 100 repetitions). All estimates were computed with the Information Breakdown Toolbox [39].

Spectral information simulation

We performed a simulation to investigate the relationship and possible dependency of the f_{MIF} from the beta frequency modulation between the STAND and WALK condition. We generated different PSDs describing beta peaks with frequency shifts varying in the range ±10Hz. First, we modeled the average power distribution μ(f). To do so, having performed a PSD parameterization, we could estimate the power at each frequency bin f as the sum of N gaussian functions. For simplicity, we assumed N = 1 and considered the highest parameterized PSD peak. Doing so, for two ideal states s_1 and s_2 we could model the mean power μ(f) as (Eqn. 4):

$$\mu(\mathrm{f}) = A_k \exp\left(-\frac{(\mathrm{f} - f_k)^2}{2\xi_k^2} \right), \quad k = s_1, s_2 \tag{4}$$

for which we could set the amplitude (A_{s_i} and A_{s_2}), the frequency peak (f_{s_1} and f_{s_2}) and the standard deviation (ξ_{s_i} and ξ_{s_2}). Then we used the maximum likelihood estimation to find μ and σ for each frequency bin in the range [5;40]Hz, for each condition and for each hemisphere (STN- and STN+). We combined all the (μ, σ) pairs and performed a linear regression analysis to find the parameters *m* and *q* of the line best fitted to their distribution. We then estimated the standard deviation σ(f) as a linear function of a known mean power μ(f) (Eqn. 5):

$$\sigma(\mathrm{f}) = m\,\mu(\mathrm{f}) + q \tag{5}$$

for each frequency f (Supp. Fig. 2).

Finally, we computed the spectral information from the three probability functions of Equation (1) (i.e., state probability *P(s)*, conditional probability *P(r|s)*, and feature probability *P(r)*) that could now be determined from the distribution of the resulting PSD values.

Classification

We used a binary (two-class) logistic regression (LR)-based classifier for classification of the STAND and WALK conditions, based on a linear combination of features extracted from preprocessed LFP. LR is widely used for classification in machine learning, and is a special case of a generalized linear model that allows easy interpretation of the results. Generally, a logistic regression defines the membership probability for one of two classes, c_1 and c_2, in the data set as $P(c_1|x,\alpha) = g(h_\alpha(x))$ and $P(c_2|x,\alpha) = 1 - P(c_1|x,\alpha)$, where $h_\alpha(x)$ is a linear function representing a weighted sum of different features $h_\alpha(x) = \alpha_0 + \alpha_1 x_1 + \alpha_2 x_2 + \ldots + \alpha_N x_N$, where x_N and α_N represent the N^{th} feature and parameter respectively, and $g(\cdot)$ is the sigmoid function used to limit the output of the linear function to the range [0;1].

The objective of the LR-based classification is to find the set of parameters α that provides the hyperplane (or decision boundary), satisfying the equation $h_\alpha(x) = 0$ and optimally separating the two classes. In LR analysis, we used as predictor variables the scalar features introduced for the information analysis, i.e., f_{PEAK}, P_{SF}, P_{WF}, P_{BETA}, and P_{MIF}.

We evaluated the performance of decoding between STAND and WALK of different LR models, based either on one single feature or on pairs, considering each hemisphere separately or both hemispheres jointly. A leave-one-out cross validation was used. Since the number of STAND and WALK epochs differed for each subject, we decided to perform the validation for 100 subsamples of epochs built as follows: (1) we randomly selected without replacement a number *N* of STAND epochs equal to the number of available WALK epochs; (2) we merged the two sets to create a single dataset with *2N* epochs. Of note, a leave-one-out cross validation was used for each subsample.

To evaluate the classification rate of the classifiers, the performance (expressed as percentage of epochs that was accurately detected as STAND or WALK) were quantified and presented. The performance reported in the results is the average across the 100 subsamples.

The performance was evaluated also in terms of accuracy and sensitivity-specificity in the ROC space plotting the ROC curve, and measuring the AUC. The ROC curve plots the true positive rate (sensitivity) against false positive rate (1-specificity) for different thresholds. The AUC provides a measure of the ability of the classifier to distinguish between the two states, with 0.5 indicating a chance-level accuracy and 1 suggesting perfect classification.

Data availability

The data sets generated during and/or analysed during the current study are available from the corresponding author on reasonable request.

Results

We recorded LFP in the STN of eight patients with PD as they executed a gait task, using a novel DBS device that allows on-demand recording of subthalamic neural activity from the chronically-implanted electrodes months after the surgical procedure. Demographic and clinical data are listed in Table 1. Values are presented as median [range]. All patients showed a sustained improvement from DBS, further supporting the correct placement of the electrodes that were used for the recording the neural activity (Table 1).

In comparison with healthy controls, all patients showed a significant bilateral reduction of striatal DAT binding ($p < 0.001$, Wilcoxon signed rank test [WSRT]). In each patient we identified one hemisphere (H) more dopamine-depleted than the opposite one (H-: 70 ± 10%; H+: 60 ± 12%). The individual values of striatal DAT binding were reported in Supp. Table 1. The clinically most impaired body side corresponded in each patient to the striatum with less non-displaceable binding potential (BP_{ND}) of DAT. We analysed separately the most and least dopamine-depleted hemisphere (STN- and STN+, respectively).

With respect to healthy control subjects, parkinsonian patients showed reduced stride length and average stride velocity, but normal stride duration, stance duration and double support duration. The individual kinematic values were reported for all patients in Supp. Table 2.

Frequency modulation of beta oscillatory activity informs about the standing vs. walking condition

We compared the LFP recordings between the STAND and WALK condition (see Methods). LFP power spectral density (PSD) displayed a distinctive frequency peak for each condition (f_{STAND} and f_{WALK}) within the beta band [13;35,]Hz (Fig. 1). The epoch wise frequency peak (f_{PEAK}) shifted towards higher frequencies from STAND to WALK in all the STN- (f_{PEAK} shift 3.6 [0.68; 8.06]Hz; $p = 0.01$, WSRT) (Fig. 2A). For the STN+, we found a positive f_{PEAK} shift in five out of eight patients (f_{PEAK} shift 2.45 [-4.16; 16.34]Hz; $p = 0.46$, WSRT) (Fig. 2A).

Table 1
Clinical and demographic data.
Patients were evaluated with the UPDRS-III within one month prior to surgery (pre-DBS) after overnight (>12 h) suspension of all dopaminergic drugs (meds-off) and upon receiving 1 to 1.5-times (range:200–300 mg) the levodopa-equivalent of the morning dose (meds-on). After surgery (post-DBS), patients were also assessed with the UPDRS-III in four conditions: (i) stimulation off for at least 2 h (stim-off); (ii) bilateral STN stimulation (stim-on); (iii) meds-on (as pre-DBS); (iv) meds-on and stim-on. Wue11 was the only female patient. DBS, deep brain stimulation; LEDD, levodopa equivalent daily dose; STN, subthalamic nucleus; UPDRS-III, Unified Parkinson Disease Rating.

Subject	Age (years)	Disease duration (years)	LEDD (mg		UPDRS-III (score)					
			pre-DBS	post-DBS	pre-DBS		post-DBS			
					meds-off	meds-on	meds-off		meds-on	
							stim-off	stim-on	stim-off	stim-on
wue02	65	10	1100	800	40	23	39	19	17	16
wue03	61	18	2725	600	40	9	45	17	23	14
wue04	54	7	658	400	26	8	27	5	9	8
wue06	51	11	1133	180	46	11	48	12	11	6
wue07	61	10	650	220	43	24	29	15	8	9
wue09	55	19	1200	730	50	11	33	16	8	11
wue10	56	10	1200	550	69	14	65	25	20	5
wue11	53	11	1300	460	55	4	51	9	13	14

The average power of the LFP in the beta band (P_{BETA}) did not show a significant modulation between STAND and WALK for both STN- (Cohen's d = 0.61, p = 0.15, WSRT) and STN+ (Cohen's d = 0.34, p = 0.31, WSRT) (Fig. 2B). No significant difference was found when computing the power relative to the range f_{STAND}±2 Hz (P_{SF}, see Methods) for the STN- (Cohen's d = 0.57, p = 0.31, WSRT) and STN+ (Cohen's d = 0.02, p = 0.46, WSRT) (Fig. 2C). In contrast, the power relative to the range f_{WALK}±2 Hz (P_{WF}, see Methods) significantly differed between the STAND and WALK condition in both the STN- (Cohen's d = 0.82, p = 0.01, WSRT) and STN+ (Cohen's d = 0.58, p < 0.01, WSRT) (Fig. 2D).

We then computed the mutual information (see Methods) between the aforementioned spectral features and the STAND and WALK condition. The f_{PEAK} carried significant information (p < 0.05, bootstrap test) about STAND and WALK for 16 of 18 hemispheres (STN-, 0.35 [0.002; 0.83]bits; STN+, 0.35 [0.03; 0.60]bits) (Fig. 3A). Very poor information was carried by P_{BETA} (STN-, 0.05 [0.003; 0.21] bits; STN+, 0.06 [0; 0.35]bits) and was significant only in eight of 16 hemispheres (p < 0.05, bootstrap test). There were similar values for P_{SF} (STN-, 0.01 [0; 0.18]bits; STN+, 0.03 [0; 0.11]bits; p < 0.05 in 5/16 hemispheres, bootstrap test) and P_{WF} (STN-, 0.02 [0; 0.40]bits;

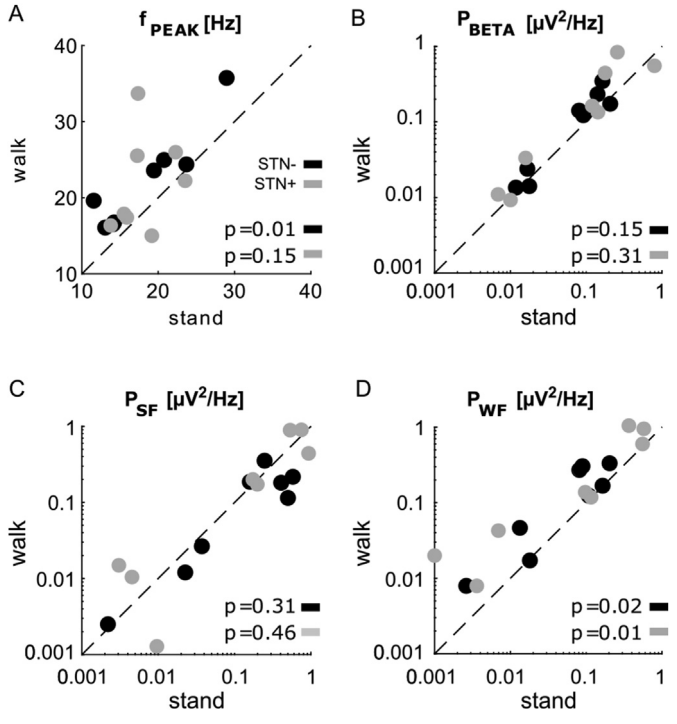

Fig. 2. Spectral differences between the standing and walking condition.
A) Comparison of median f_{PEAK} in the subthalamic local field potentials power spectral density during standing and walking for each subject. Black and grey markers indicate the most and least dopamine-depleted hemispheres of the subthalamic nucleus (STN- and STN+), respectively. The dashed line represents the identity line. Insets indicate the significance of the matched pair Wilcoxon signed rank test. **B-D)** Same as (A) for the whole beta power P_{BETA} (**B**), the power in the range f_{STAND}±2 Hz (P_{SF}) (**C**), and the power in the range f_{WALK}±2 Hz (P_{WF}) (**D**).

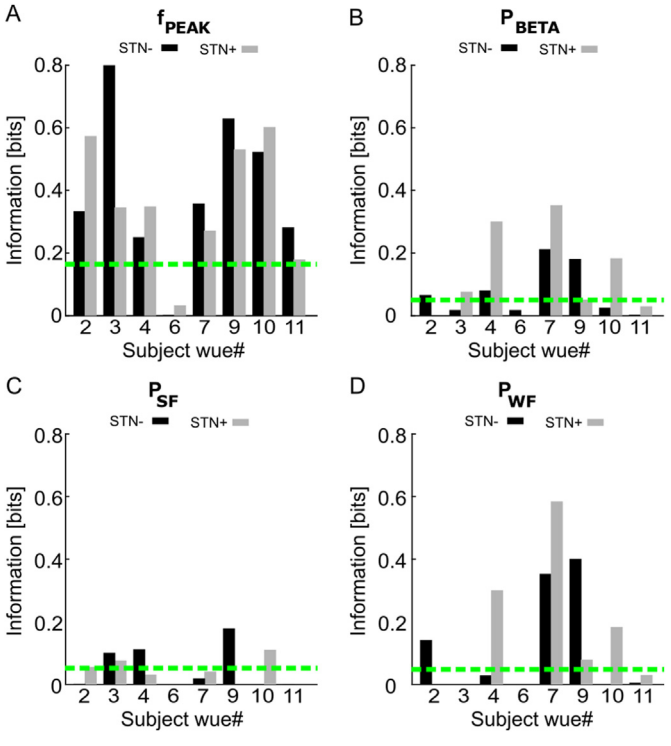

Fig. 3. Information about standing and walking carried by spectral features. A) Information carried by f_{PEAK}. Black and grey markers indicate the most and least dopamine-depleted hemispheres of the subthalamic nucleus (STN- and STN+), respectively. Green dashed lines represent the p = 0.05 significance threshold (bootstrap test). **B-D)** Same as (A) for the whole beta power P_{BETA} (**B**), the power in the range f_{STAND}±2 Hz (P_{SF}) (**C**), and the power in the range f_{WALK}±2 Hz (P_{WF}) (**D**). (For interpretation of the references to color in this figure legend, the reader is referred to the Web version of this article.)

STN+, 0.05 [0; 0.58]bits; $p < 0.05$ in 7/16 hemispheres, bootstrap test) (Fig. 3B–D). Information carried by P_{BETA}, P_{SF}, and P_{WF} was significantly less than information carried by f_{PEAK} (all $p < 0.01$, WSRT).

Striatal DAT bindings values of both STN- and STN + did not correlate with any of the aforementioned spectral features ($p > 0.3$, WSRT).

Frequency peak shift and most informative frequency

We computed a complete spectral information analysis (see Methods) and identified for each patient the most informative frequency about the WALK and STAND condition (f_{MIF}, Fig. 4A). This was typically located outside the range $]f_{STAND}$ - $f_{WALK}[$ (15/16 hemispheres, Fig. 4B). The power relative to the range $f_{MIF}\pm2$ Hz (P_{MIF}) carried significant information about STAND and WALK ($p < 0.05$ for 16/18 hemispheres, bootstrap test; STN-, 0.16 [0.04; 0.41]bits; STN+, 0.25 [0.03; 0.58]bits) (Fig. 4C). The joint knowledge of P_{MIF} in the two hemispheres led to an increase of the information (0.28 [0.14; 0.66]bits; $p < 0.05$ for 16/18 hemispheres, bootstrap test) (Fig. 4D). Of note, the joint information carried by P_{MIF} in the two hemispheres showed a redundancy of 34 [-39; 67]% (Fig. 4D).

We then simulated an ideal condition (see Methods) in which the average spectral densities over two different states differed only for the peak frequency (Fig. 5A). We implemented an inter-trial variability proportional to the power that we observed in our recordings (Supp. Fig. 2). Under these conditions, the f_{MIF} would be located outside the range within f_{STAND} and f_{WALK} for a broad range of shifts (Fig. 5B), coherent with our experimental observations.

Frequency-shift features f_{PEAK} and P_{MIF} reliably classify the standing and walking condition

We assessed the ability of the aforementioned features in discriminating between STAND and WALK with a binary logistic regression-based classifier (see Methods). When based on f_{PEAK}, the classifier discriminated between the two conditions for both hemispheres (STN-, performance 0.87 [0.58; 1], $p < 0.05$ Clopper-Pearson test (CPt) for 8/8 patients; STN+, performance 0.90 [0.68; 1], $p < 0.05$ CPt for all eight patients) (Fig. 6A top). Comparable results were obtained when the classifier was based on the P_{MIF} (STN-, performance 0.78 [0.59; 0.92], $p < 0.05$ CPt for 7/8 patients; STN+, performance 0.84 [0.71; 1], $p < 0.05$ CPt for 8/8 patients) (Fig. 6B top), which further improved when the two hemispheres were combined (performance 0.90 [0.82; 1]; $p < 0.05$ CPt for 8/8 patients) (Fig. 6C top). In line with these results, the accuracy of the decoder measured as the area under the curve (AUC) of the receiver operating characteristic (ROC) was high when based on f_{PEAK} (STN-, 0.94 [0.51; 0.95]; STN+, 0.93 [0.66; 1.00]) and P_{MIF} (STN-, 0.80 [0.55; 0.99]; STN+, 0.84 [0.61; 1.00]; combined hemispheres, 0.91 [0.60; 1.00]) (Fig. 6A–C bottom). Discriminating STAND and WALK using P_{BETA}, P_{SF} and P_{WF} led to poor performances (Supp. Fig. 3).

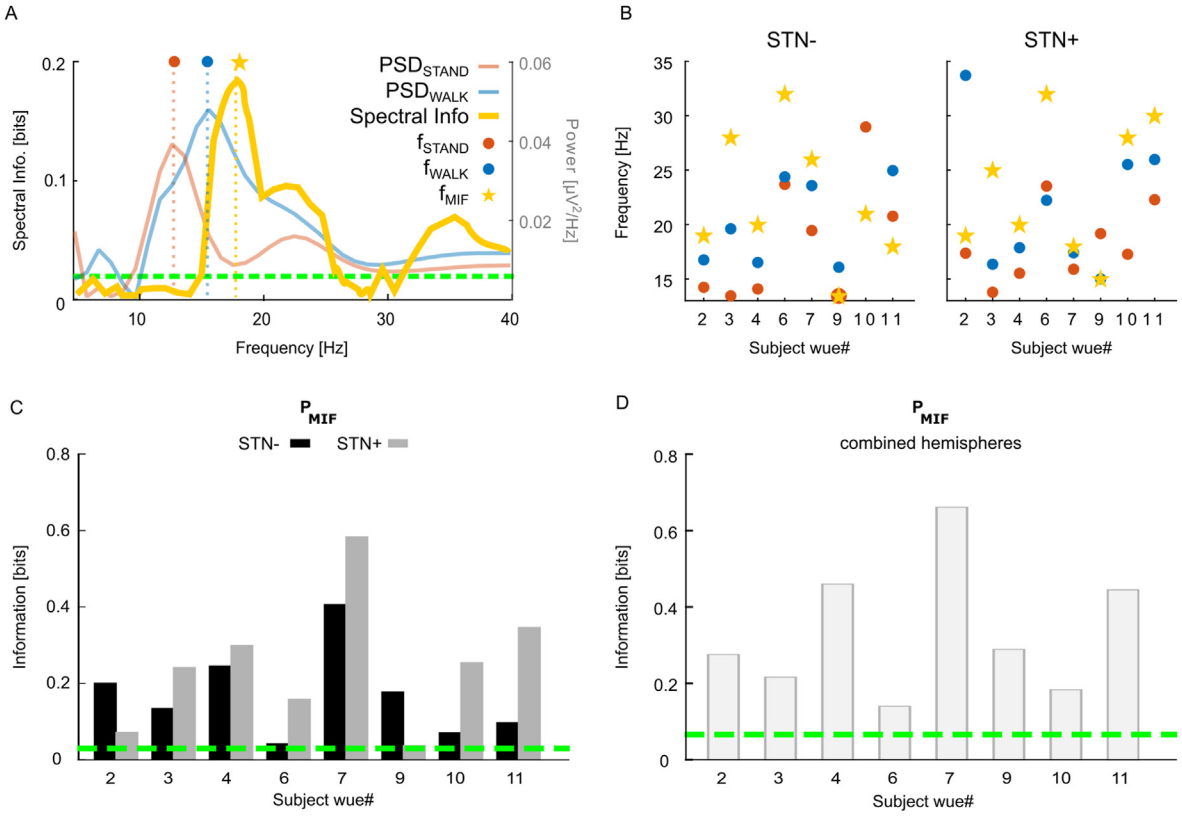

Fig. 4. Most informative frequency (f_{MIF}).
A)Spectral information (yellow line) computed for the power spectral density in standing (red line) and walking (blue lines) for the most dopamine-depleted hemisphere of the subthalamic nucleus (STN-) of patient wue02 (related to Fig. 1a). Green dashed lines represent the $p = 0.05$ significance threshold (bootstrap test). The red dot indicates the frequency peak of STAND epochs (f_{STAND}), the blue dot indicates the frequency peak of WALK epochs (f_{WALK}) and the yellow star indicates the most informative frequency (f_{MIF}). **B)** Representation of f_{STAND}, (red dot), f_{WALK} (blue dot), and the MIF (yellow star) for each subject for the STN- (left) and the STN+ (right). **C)** Information about standing and walking carried by the power in the range $f_{MIF}\pm2$ Hz (P_{MIF}) for STN- (black) and STN+ (grey) for each subject. **D)** Same as (C) combining P_{MIF} of the two hemispheres. (For interpretation of the references to color in this figure legend, the reader is referred to the Web version of this article.)

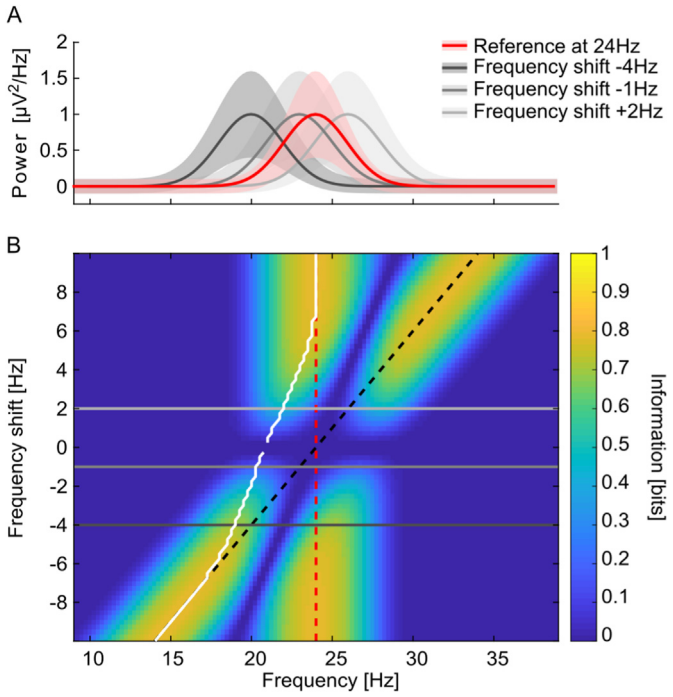

Fig. 5. Peak frequency shift and most informative frequency.
A) Simulated power spectral density (PSD) power for an ideal reference state s_1 with amplitude $A_{s_1} = 1\mu V^2/Hz$, standard deviation $\xi_{s_1} = 2Hz$, and frequency peak $f_{s_1} = 24Hz$ (red), and three conditions with same distribution but peak frequency shifts equal to -4 Hz (black line), -1 Hz (grey line), and 2 Hz (light grey line). The shaded areas represent the standard deviation (see Methods). **B)** Spectral information between s1 and a second state s_2 with frequency shift in the range [-10; 10]Hz, excluding the singular point at 0 Hz shift. Red and black dotted lines represent the location of the frequency peak, respectively, in states s_1 and s_2 PSD. White line indicates the location of the maximum of the spectral information for each frequency shift between s_1 and s_2. Black, grey, and light grey lines show the three examples of frequency shifts described in (A). (For interpretation of the references to color in this figure legend, the reader is referred to the Web version of this article.)

Discussion

Our study provides the first evidence of beta frequency modulation associated with locomotion in the STN of parkinsonian patients. Starting from this result, we performed an information theoretic analysis and we identified a maximally informative frequency (f_{MIF}) whose power (P_{MIF}) can accurately decode the walking state, with respect to upright standing, for each single patient. This marker could be used in already available aDBS devices that sense for beta power modulation to timely adjust the stimulation delivery to locomotion.

The orthograde human posture and locomotion are unique among all mammals and probably one of our most vital activities. Human gait is complex and requires a constant and coordinated flow of information across functionally-specialized brain areas, the locomotor network [20,41,42]. This network comprises several cortical areas (including the premotor, supplementary motor, and parietal areas), the basal ganglia and the STN, the mesencephalic locomotor region (MLR), the thalamus, the cerebellum, and the central pattern generators (CPG), i.e., the spinal neuronal circuit that control the basic rhythms and patterns of motor neuron activation during locomotion [20]. Each of these structures plays a specific role in gait control as part of highly coordinated independent oscillators of distinctive circuits. For example, the spinal CPG circuitry involves the stretch reflex, reciprocal and non-reciprocal inhibition, and flexion reflexes that are fundamental to generate rhythm and pattern of limb movements [20]. The STN circuitry also plays an essential role in the locomotor network [41]. It gates the integration of cortical (motor feedforward) and cerebellar (sensory feedback) information by activating or inhibiting the MLR via direct glutamatergic projection or through the basal ganglia GABAergic output nuclei (i.e., the GPi and the substantia nigra pars reticulate [SNr]). The STN is the cornerstone that gears up the locomotor network. Indeed, failure of cortical-subthalamic information processing in parkinsonian patients can result in an abrupt interruption of locomotion (freezing of gait) [24].

Very few studies have recorded the timely activity of the STN in PD during actual gait. In particular, Quinn and coll [43]. showed a reduced subthalamic beta power during walking with respect to standing in akinetic-rigid parkinsonian patients. A reduced high beta band [20;30]Hz power during normal and slow gait with respect to standing was also reported by Hell and coll [44]. However, Syrkin-Nikolau and coll. and Arnulfo and coll. showed similar subthalamic beta power during standing and walking [21,45]. All these studies were performed in chronically-implanted PD patients with the same device (i.e., Activa PC+S®, Medtronic PLC), and all patients experienced a sustained benefit from DBS, thus supporting a correct clinical diagnosis and proper placement of the electrodes used for stimulation and recording of the STN neural activity. The discrepancy in results cannot rely solely on different methodological approaches, but instead suggests other domains than amplitude modulation for the coding of locomotion at an STN level.

As previously suggested by Priori and coll. [18,46], frequency modulation (FM) could be an alternative modality to effectively convey the information flow across multiple, weakly connected circuits (autonomous oscillators, e.g., CPG, thalamocortical-basal ganglia, etc.) of a large-scale network such as the locomotor network [47,48]. Accordingly, local brain circuits would tune their endogenous frequency (rhythms) to engage a variety of phase relationships within a functional network, routing task-related information toward relevant neural targets [16,17]. Such a communication through frequency- and phase-specific synchronization has been previously described for alpha frequency oscillations in cognitive and sensorimotor processing, including postural maintenance [19,49], and now also for the first time in the beta band recordings of the STN of parkinsonian patients.

In the context of PD, our understanding of circuit-specific alterations and their reflection at a network level is still at its prime. On one hand, we notice symptom-specific (and dopamine-dependent) circuit oscillatory derangements [24]; on the other, we can envision the presence of physiologically preserved or compensatory circuits dynamics capable of restoring, at least temporarily, proper network functioning. Indeed, PD clinically manifests upon a loss of approximately 30% of substantia nigra pars compacta neurons and 50%–70% of dopaminergic markers in the striatum [50,51]. In line, we did not observe any correlation or dependency between beta power or frequency modulation and striatal DAT density. Together with the relatively preserved kinematics measurements of our patients (Supp. Table 2), these findings would suggest a neurophysiological relevance of subthalamic FM in human locomotion. Future studies with multiple complementary investigations (e.g., EEG, ^{18}F-Dopa PET) in patients with different neurological disorders might confirm this assumption.

Our study provides an innovative approach to extract more robust biomarkers encoding ongoing tasks execution intervals. Until now, research has aimed to identify electrophysiological biomarkers targeting symptom-specific causal pathological mechanisms within the implanted brain area (e.g., the STN). However, these biomarkers, such as beta power [52], might not accurately capture task-related dynamics at a circuitry level, especially when coded in the frequency domain [18,19]. Indeed, we showed that even when reaching statistical significance across subjects, subthalamic power

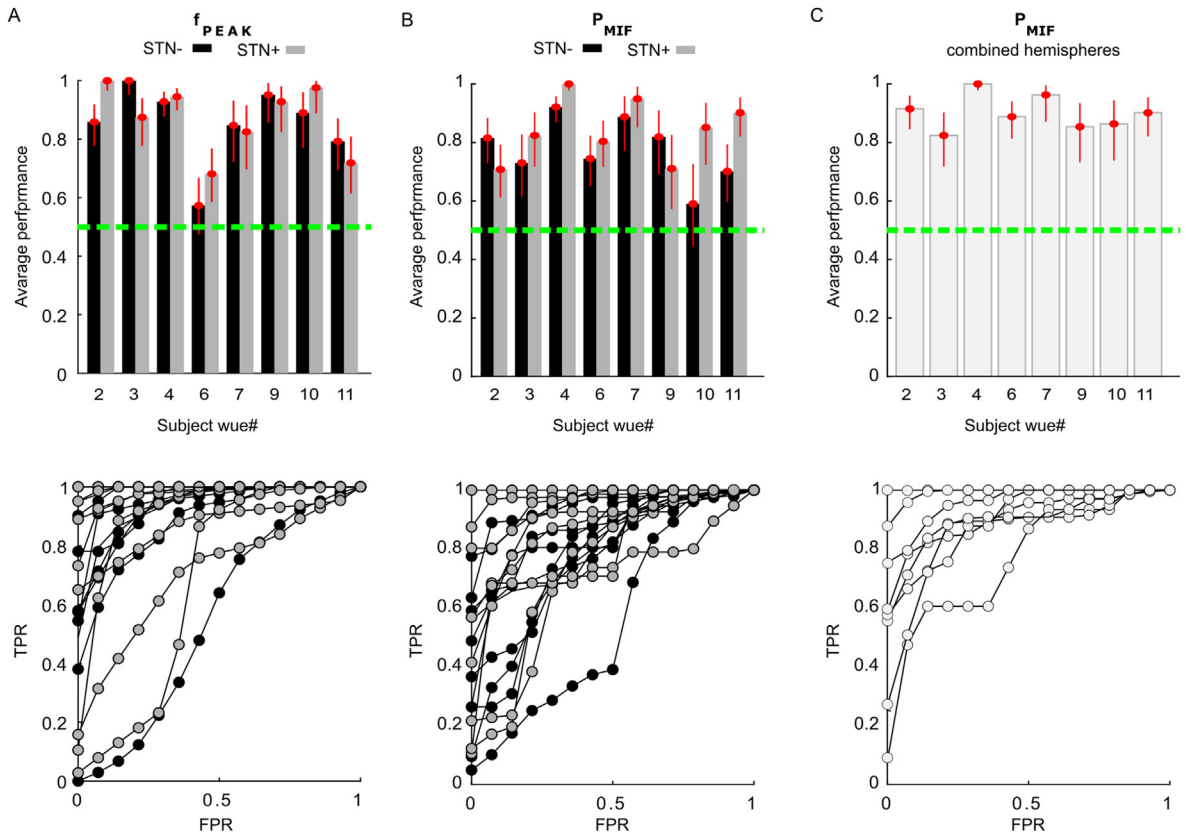

Fig. 6. Linear regression classifier based on features related to peak-frequency shift.
A) (top) Average performance in discriminating between standing and walking for a logistic regression binary classifier, based on the f_{PEAK} for the least and most dopamine-depleted hemispheres of the subthalamic nucleus (STN- (black) and STN+ (grey), respectively) for each subject. The green dashed line indicates 50% chance level. Vertical red error bars indicate the 5% and the 95% Clopper-Pearson Binomial proportion confidence interval. **(bottom)** Receiver operating characteristic curves showing, for STN- (black) and STN+ (grey) of each subject, the trade-off between false positive rates (FPR) and true positive rates (TPR) of the logistic regression classifier for f_{PEAK}. **B–C)** Same as (A) for the power in the range f_{MIF}±2 Hz (P_{MIF}) **B)** and for the combination of the P_{MIF} of the two hemispheres **C)**, respectively. . (For interpretation of the references to color in this figure legend, the reader is referred to the Web version of this article.)

modulations may carry scarce gait-related information due to intra-subject variability (such as P_{WF}, see Figs. 2D and 3D), rendering them unable to properly discriminate the walking condition (Supp. Fig. 3). Of relevance, the use of a suboptimal biomarker could be detrimental, possibly interfering with the FM needed for the transition from upright quiet standing to steady state walking [15].

In this context, spectral and mutual information analysis of subthalamic LFP recordings is a valuable aid to identify maximally informative frequencies whose power changes reflect tasks execution. This approach could be readily tested in available aDBS devices (intended to monitor power changes rather than frequency modulations), to promptly activate stimulation parameters more effective for locomotion (e.g., 60Hz) [53,54]. This approach can also reduce the number of task-specific frequencies to be monitored by aDBS devices (i.e. P_{MIF} instead of f_{PEAK} shift or f_{STAND} and f_{WALK}). Finally, our simulation study shows that the f_{MIF} is a direct consequence of the shift of the frequency peak in the beta range. It should be highlighted that this implies that (i) these results are not related to any oscillation occurring in the basal ganglia network with frequency f_{MIF}, (ii) ideally, f_{MIF} matches with f_{STAND} and f_{WALK} only for very large peak frequency shifts (Fig. 5B), and (iii) as the peak frequency shift is patient-specific f_{MIF} differs between patients. Preliminary recording sessions of different motor and non-motor tasks should therefore be envisioned to identify multiple patient- and task-specific f_{MIF} for aDBS devices.

In conclusion, we have provided preliminary evidence of gait-related beta-frequency modulation in the STN of parkinsonian patients. Highly-sensitive metrics (i.e., f_{MIF} and P_{MIF}) can enrich the spectrum of symptom-based biomarkers, with input signals encoding ongoing tasks execution for an appropriate tuning of DBS parameters.

Author contributions

AC: Methodology, Formal analysis, Writing, Visualization; CP: Methodology, Formal analysis, Investigation, Data curation; IUI: Conceptualization, Methodology, Formal analysis, Investigation, Resources, Writing, Visualization, Supervision, Project administration, Funding acquisition; AM: Methodology, Formal analysis, Writing, Visualization, Supervision.

Funding

The study was sponsored in part by the Deutsche Forschungsgemeinschaft (DFG, German Research Foundation) – Project-ID 424778381 – TRR 295 and the “Fondazione Grigioni per il Morbo di Parkinson”. AC was supported by a grant from the Fondazione Europea di Ricerca Biomedica (FERB Onlus).

Declaration of competing interest

The authors declare that the research was conducted in the absence of any commercial or financial relationships that could be construed as a potential conflict of interest. The Activa PC+S®

system and the related hardware and software for programming and readout were provided under a request for application agreement by Medtronic, PLC. The companies had no impact on study design, patient selection, data analysis, or reporting of the results.

Acknowledgements

The authors would like to thank Prof. C. Matthies for the neurosurgical information, Dr. J. Brumberg and Dr. N. G. Pozzi for their help with data acquisition, and Mr. M. Vissani for suggestions about the data analysis.

Appendix A. Supplementary data

Supplementary data to this article can be found online at https://doi.org/10.1016/j.brs.2020.09.006.

References

[1] Defebvre L, Blatt J-L, Blond S, Bourriez J-L, Guieu J-D, Destée A. Effect of thalamic stimulation on gait in Parkinson disease. Arch Neurol 1996;53:898–903. https://doi.org/10.1001/archneur.1996.00550090108016.
[2] Pötter-Nerger M, Volkmann J. Deep brain stimulation for gait and postural symptoms in Parkinson's disease. Mov Disord 2013;28:1609–15. https://doi.org/10.1002/mds.25677.
[3] Schrader C, Capelle H-H, Kinfe TM, Blahak C, Bäzner H, Lütjens G, et al. GPi-DBS may induce a hypokinetic gait disorder with freezing of gait in patients with dystonia. Neurology 2011;77:483–8. https://doi.org/10.1212/WNL.0b013e318227b19e.
[4] Reich MM, Brumberg J, Pozzi NG, Marotta G, Roothans J, Åström M, et al. Progressive gait ataxia following deep brain stimulation for essential tremor: adverse effect or lack of efficacy? Brain 2016;139:2948–56. https://doi.org/10.1093/brain/aww223.
[5] Little S, Pogosyan A, Neal S, Zavala B, Zrinzo L, Hariz M, et al. Adaptive deep brain stimulation in advanced Parkinson disease. Ann Neurol 2013;74:449–57. https://doi.org/10.1002/ana.23951.
[6] Arlotti M, Marceglia S, Foffani G, Volkmann J, Lozano AM, Moro E, et al. Eight-hours adaptive deep brain stimulation in patients with Parkinson disease. Neurology 2018;90:e971–6. https://doi.org/10.1212/WNL.0000000000005121.
[7] Arlotti M, Palmisano C, Minafra B, Todisco M, Pacchetti C, Canessa A, et al. Monitoring subthalamic oscillations for 24 hours in a freely moving Parkinson's disease patient. Mov Disord 2019;34:757–9. https://doi.org/10.1002/mds.27657.
[8] Neumann W-J, Staub-Bartelt F, Horn A, Schanda J, Schneider G-H, Brown P, et al. Long term correlation of subthalamic beta band activity with motor impairment in patients with Parkinson's disease. Clin Neurophysiol 2017;128:2286–91. https://doi.org/10.1016/j.clinph.2017.08.028.
[9] Kühn AA, Kupsch A, Schneider G-H, Brown P. Reduction in subthalamic 8–35 Hz oscillatory activity correlates with clinical improvement in Parkinson's disease. Eur J Neurosci 2006;23:1956–60. https://doi.org/10.1111/j.1460-9568.2006.04717.x.
[10] Kühn AA, Kempf F, Brücke C, Gaynor Doyle L, Martinez-Torres I, Pogosyan A, et al. High-frequency stimulation of the subthalamic nucleus suppresses oscillatory beta activity in patients with Parkinson's disease in parallel with improvement in motor performance. J Neurosci 2008;28:6165–73. https://doi.org/10.1523/JNEUROSCI.0282-08.2008.
[11] Chen CC, Hsu YT, Chan HL, Chiou SM, Tu PH, Lee ST, et al. Complexity of subthalamic 13–35Hz oscillatory activity directly correlates with clinical impairment in patients with Parkinson's disease. Exp Neurol 2010;224:234–40. https://doi.org/10.1016/j.expneurol.2010.03.015.
[12] Little S, Pogosyan A, Kuhn AA, Brown P. Beta band stability over time correlates with Parkinsonian rigidity and bradykinesia. Exp Neurol 2012;236:383–8. https://doi.org/10.1016/j.expneurol.2012.04.024.
[13] Beudel M, Oswal A, Jha A, Foltynie T, Zrinzo L, Hariz M, et al. Oscillatory beta power correlates with akinesia-rigidity in the parkinsonian subthalamic nucleus. Mov Disord 2017;32:174–5. https://doi.org/10.1002/mds.26860.
[14] Schmidt R, Ruiz MH, Kilavik BE, Lundqvist M, Starr PA, Aron AR. Beta oscillations in working memory, executive control of movement and thought, and sensorimotor function. J Neurosci 2019;39:8231–8. https://doi.org/10.1523/JNEUROSCI.1163-19.2019.
[15] Iturrate I, Martin S, Chavarriaga R, Orset B, Leeb R, Sobolewski A, et al. Beta-driven closed-loop deep brain stimulation can compromise human motor behavior in Parkinson's Disease. BioRxiv 2019:696385. https://doi.org/10.1101/696385.
[16] Fries P. Rhythms for cognition: communication through coherence. Neuron 2015;88:220–35. https://doi.org/10.1016/j.neuron.2015.09.034.
[17] Fries P. A mechanism for cognitive dynamics: neuronal communication through neuronal coherence. Trends Cognit Sci 2005;9:474–80. https://doi.org/10.1016/j.tics.2005.08.011.
[18] Foffani G, Bianchi A, Baselli G, Priori A. Movement-related frequency modulation of beta oscillatory activity in the human subthalamic nucleus. J Physiol 2005;568:699–711. https://doi.org/10.1113/jphysiol.2005.089722.
[19] Mierau A, Klimesch W, Lefebvre J. State-dependent alpha peak frequency shifts: experimental evidence, potential mechanisms and functional implications. Neuroscience 2017;360:146–54. https://doi.org/10.1016/j.neuroscience.2017.07.037.
[20] Takakusaki K. Functional neuroanatomy for posture and gait control. J Mov Disord 2017;10:1–17. https://doi.org/10.14802/jmd.16062.
[21] Arnulfo G, Pozzi NG, Palmisano C, Leporini A, Canessa A, Brumberg J, et al. Phase matters: a role for the subthalamic network during gait. PloS One 2018;13:e0198691. https://doi.org/10.1371/journal.pone.0198691.
[22] Hughes AJ, Daniel SE, Ben-Shlomo Y, Lees AJ. The accuracy of diagnosis of parkinsonian syndromes in a specialist movement disorder service. Brain 2002;125:861–70. https://doi.org/10.1093/brain/awf080.
[23] Steigerwald F, Pötter M, Herzog J, Pinsker M, Kopper F, Mehdorn H, et al. Neuronal activity of the human subthalamic nucleus in the parkinsonian and nonparkinsonian state. J Neurophysiol 2008;100:2515–24. https://doi.org/10.1152/jn.90574.2008.
[24] Pozzi NG, Canessa A, Palmisano C, Brumberg J, Steigerwald F, Reich MM, et al. Freezing of gait in Parkinson's disease reflects a sudden derangement of locomotor network dynamics. Brain 2019;142:2037–50. https://doi.org/10.1093/brain/awz141.
[25] Isaias IU, Benti R, Goldwurm S, Zini M, Cilia R, Gerundini P, et al. Striatal dopamine transporter binding in Parkinson's disease associated with the LRRK2 Gly2019Ser mutation. Mov Disord 2006;21:1144–7. https://doi.org/10.1002/mds.20909.
[26] Isaias IU, Alterman RL, Tagliati M. Outcome predictors of pallidal stimulation in patients with primary dystonia: the role of disease duration. Brain 2008;131. https://doi.org/10.1093/brain/awn120. 1895–902.
[27] Palmisano C, Brandt G, Vissani M, Pozzi NG, Canessa A, Brumberg J, et al. Gait initiation in Parkinson's disease: impact of dopamine depletion and initial stance condition. Front Bioeng Biotechnol 2020;8. https://doi.org/10.3389/fbioe.2020.00137.
[28] Isaias IU, Volkmann J, Marzegan A, Marotta G, Cavallari P, Pezzoli G. The influence of dopaminergic striatal innervation on upper limb locomotor synergies. PloS One 2012;7:e51464. https://doi.org/10.1371/journal.pone.0051464.
[29] Devos D, Szurhaj W, Reyns N, Labyt E, Houdayer E, Bourriez JL, et al. Predominance of the contralateral movement-related activity in the subthalamo-cortical loop. Clin Neurophysiol 2006;117:2315–27. https://doi.org/10.1016/j.clinph.2006.06.719.
[30] Canessa A, Pozzi NG, Arnulfo G, Brumberg J, Reich MM, Pezzoli G, et al. Striatal dopaminergic innervation regulates subthalamic beta-oscillations and cortical-subcortical coupling during movements: preliminary evidence in subjects with Parkinson's disease. Front Hum Neurosci 2016;10. https://doi.org/10.3389/fnhum.2016.00611.
[31] Torrence C, Compo GP. A practical guide to wavelet analysis. Bull Am Meteorol Soc 1998;79:18.
[32] Sadeghi H, Allard P, Shafie K, Mathieu PA, Sadeghi S, Prince F, et al. Reduction of gait data variability using curve registration. Gait Posture 2000;12:257–64. https://doi.org/10.1016/S0966-6362(00)00085-0.
[33] Haller M, Donoghue T, Peterson E, Varma P, Sebastian P, Gao R, et al. Parameterizing neural power spectra. Neuroscience 2018. https://doi.org/10.1101/299859.
[34] Shannon CE. A mathematical theory of communication. Bell Sys Tech J 1948;27:379–423.
[35] Mazzoni A, Brunel N, Cavallari S, Logothetis NK, Panzeri S. Cortical dynamics during naturalistic sensory stimulations: experiments and models. J Physiol Paris 2011;105:2–15. https://doi.org/10.1016/j.jphysparis.2011.07.014.
[36] Panzeri S, Petroni F, Petersen RS, Diamond ME. Decoding neuronal population activity in rat somatosensory cortex: role of columnar organization. Cereb Cortex 2003;13:45–52. https://doi.org/10.1093/cercor/13.1.45.
[37] Belitski A, Gretton A, Magri C, Murayama Y, Montemurro MA, Logothetis NK, et al. Low-frequency local field potentials and spikes in primary visual cortex convey independent visual information. J Neurosci 2008;28:5696–709. https://doi.org/10.1523/JNEUROSCI.0009-08.2008.
[38] Mazzoni A, Panzeri S, Logothetis NK, Brunel N. Encoding of naturalistic stimuli by local field potential spectra in networks of excitatory and inhibitory neurons. PLoS Comput Biol 2008;4:e1000239. https://doi.org/10.1371/journal.pcbi.1000239.
[39] Magri C, Whittingstall K, Singh V, Logothetis NK, Panzeri S. A toolbox for the fast information analysis of multiple-site LFP, EEG and spike train recordings. BMC Neurosci 2009;10:81. https://doi.org/10.1186/1471-2202-10-81.
[40] Panzeri S, Treves A. Analytical estimates of limited sampling biases in different information measures. Netw Comput Neural Syst 1996;7:87–107. https://doi.org/10.1080/0954898X.1996.11978656.
[41] la Fougère C, Zwergal A, Rominger A, Förster S, Fesl G, Dieterich M, et al. Real versus imagined locomotion: a [18F]-FDG PET-fMRI comparison. Neuroimage 2010;50:1589–98. https://doi.org/10.1016/j.neuroimage.2009.12.060.
[42] Jahn K, Deutschländer A, Stephan T, Kalla R, Wiesmann M, Strupp M, et al. Imaging human supraspinal locomotor centers in brainstem and cerebellum.

Neuroimage 2008;39:786–92. https://doi.org/10.1016/j.neuroimage.2007.09.047.
[43] Quinn EJ, Blumenfeld Z, Velisar A, Koop MM, Shreve LA, Trager MH, et al. Beta oscillations in freely moving Parkinson's subjects are attenuated during deep brain stimulation. Mov Disord 2015;30:1750–8. https://doi.org/10.1002/mds.26376.
[44] Hell F, Plate A, Mehrkens JH, Bötzel K. Subthalamic oscillatory activity and connectivity during gait in Parkinson's disease. Neuroimage: Clinical 2018;19:396–405. https://doi.org/10.1016/j.nicl.2018.05.001.
[45] Syrkin-Nikolau J, Koop MM, Prieto T, Anidi C, Afzal MF, Velisar A, et al. Subthalamic neural entropy is a feature of freezing of gait in freely moving people with Parkinson's disease. Neurobiol Dis 2017;108:288–97. https://doi.org/10.1016/j.nbd.2017.09.002.
[46] Priori A, Foffani G, Pesenti A, Tamma F, Bianchi AM, Pellegrini M, et al. Rhythm-specific pharmacological modulation of subthalamic activity in Parkinson's disease. Exp Neurol 2004;189:369–79. https://doi.org/10.1016/j.expneurol.2004.06.001.
[47] Izhikevich EM. Weakly connected quasi-periodic oscillators, FM interactions, and multiplexing in the brain. SIAM J Appl Math 1999;59:2193–223. https://doi.org/10.1137/S0036139997330623.
[48] Hoppensteadt FC, Izhikevich EM. Thalamo-cortical interactions modeled by weakly connected oscillators: could the brain use FM radio principles? Biosystems 1998;48:85–94. https://doi.org/10.1016/S0303-2647(98)00053-7.
[49] Hülsdünker T, Mierau A, Strüder HK. Higher balance task demands are associated with an increase in individual alpha peak frequency. Front Hum Neurosci 2016;9. https://doi.org/10.3389/fnhum.2015.00695.
[50] Schwarz J, Storch A, Koch W, Pogarell O, Radau PE, Tatsch K. Loss of dopamine transporter binding in Parkinson's disease follows a single exponential rather than linear decline. J Nucl Med 2004;45:1694–7.
[51] Greffard S, Verny M, Bonnet A-M, Beinis J-Y, Gallinari C, Meaume S, et al. Motor score of the Unified Parkinson Disease Rating Scale as a good predictor of Lewy body-associated neuronal loss in the substantia nigra. Arch Neurol 2006;63:584–8. https://doi.org/10.1001/archneur.63.4.584.
[52] Kühn AA, Tsui A, Aziz T, Ray N, Brücke C, Kupsch A, et al. Pathological synchronisation in the subthalamic nucleus of patients with Parkinson's disease relates to both bradykinesia and rigidity. Exp Neurol 2009;215:380–7. https://doi.org/10.1016/j.expneurol.2008.11.008.
[53] Moreau C, Defebvre L, Destée A, Bleuse S, Clement F, Blatt JL, et al. STN-DBS frequency effects on freezing of gait in advanced Parkinson disease. Neurology 2008;71:80–4. https://doi.org/10.1212/01.wnl.0000303972.16279.46.
[54] Xie T, Vigil J, MacCracken E, Gasparaitis A, Young J, Kang W, et al. Low-frequency stimulation of STN-DBS reduces aspiration and freezing of gait in patients with PD. Neurology 2015;84:415–20. https://doi.org/10.1212/WNL.0000000000001184.